The 2013 World Congress on
Advances in Structural Engineering and Mechanics (ASEM13)
Jeju, Korea, September 8-12, 2013

Numerical modeling of shock generation and propagation during satellite separation

*Marshal Deep Kafle[1)], Dae-Oen Lee[1)], Juho Lee[1)],
Jae-Hung Han[2)] and Sung-Hyun Woo[3)]

[1), 2)] *Department of Aerospace Engineering, KAIST, Daejeon 305-701, Korea*
[3)] *Korea Aerospace Research Institute, Daejeon 305-333, Korea*
[2)] *jaehunghan@kaist.ac.kr*

ABSTRACT

Various kinds of pyrotechnic devices such as explosive bolts, jet cord, pin pushers etc. are used in aerospace structure during many space missions. During their operation, these devices generate pyrotechnic shock which have very strong acceleration level at high frequency and can fail the mission equipment installed on the structure. Therefore, the estimation of shock response induced by these pyrotechnic devices is essential for success of the corresponding space program. In the present study, a clamp band system with a pyrotechnic device that separates the satellite from the launch vehicle is considered. Numerical program like Ansys-Explicit Dynamics and AUTODYN are jointly utilized to analyze the shock generation and Statistical Energy Analysis (SEA) along with Virtual Mode Synthesis (VMS) methods are applied to predict the shock propagation during satellite separation. The results obtained are evaluated and several conclusions are drawn.

1 INTRODUCTION

Today's aerospace vehicles utilize numerous pyrotechnic devices to separate structural subsystems, deploy appendages and activate on board operational subsystems. The firing of these pyrotechnical charges generates severe impulsive loads that can cause failures in electronic components. These impulsive load or called pyrotechnic shock is a transient motion of structural element, assemblies, subsystems or systems due to explosive loading induced by the detonation of ordnance devices incorporated into or attached to the structure. Pyroshock is often characterized by its high peak acceleration (300g~300kg), high frequency content (100Hz~1MHz) and short duration (10μsec to 20msec), which is largely dependent on the source type and strength, structural type and configuration, and especially the distance from the source to the response point of interest as referred by (NASA 1996). (Walter 2006) mentioned

[1)] Graduate Student
[2)] Professor
[3)] Researcher

that with the passing of time, electrical and optical components have become increasingly more miniature and because of this miniaturization the mechanical resonant frequencies of these components have increased making them susceptible to damage by pyroshock. Several flight items are sensitive to these shock and their failures could led to catastrophic mission loss.

Till now, it is very difficult for engineers, technicians, designers and students to solve problems associated with design, development, testing and evaluation of the pyrotechnic device and system. As a result, these devices could only be qualified by a very extensive, costly series of experiments. As there are not many information regarding design and analysis of such kinds of device to perform any numerical study and thus it is very hard to obtain accurate results. The design of such pyrotechnic devices/explosive bolts requires careful consideration of design factors like firing characteristics, shape, size and kind of explosive bolts, quantity of explosive material and environmental condition to ensure clean separation without fragmentation and with minimum pyroshock as indicated by (Lee 2004). The dynamic of such device is highly non-linear due to material/structural behavior and/or explosion wave and its interaction with structure during their operation. Therefore, to simulate the explosion environment and perform behavior analysis is highly challenging. Several researchers tried numerous numerical techniques to study such highly non-linear dynamic problems. The term high frequency simply implies that the number of repetitions per unit time of a complete waveform is many times the natural frequency of a system. When dealing with higher order mode analysis, deterministic analysis of individual modes becomes less successful and more difficult. The reason for this is due to basic uncertainty in modal parameters in higher order modes. As frequency increases, resonance frequencies and mode shapes become more sensitive to small details in structure's geometry, boundary conditions and damping distribution so that it is hard to predict them reliably even in nominally identical structures due to unavoidable uncertainty concerning structure details and material properties associated with manufacturing tolerances and fabrication imperfections. Furthermore, all the modes group together in frequency so that the response of all systems at any particular frequency comprises contributions from an increasing number of modes resulting in unpredictably different behavior of similar structural dynamic and acoustic systems. Thus, the prediction using other technique like finite element method (FEM) and boundary element method (BEM) becomes meaningless in higher frequency domain. The pyroshock environment for the space satellite system is generally assessed by empirical approaches using the test result of the previous similar structure. However, since the accuracy of the result is strongly related to the structural geometry, it has been predicted that those approaches are not sufficient to estimate the pyroshock environment for the future space structures.

In this paper, the response of the satellite to high frequency load due to activation of pyrotechnic device for separation of satellite from its launch vehicle is predicted. Generally, clamp band system has been used to separate satellite from their boosters as referred by (Chang 2002) and this uses one of the pyrotechnic devices for separation of space satellites from a launcher in space as cited by (Iwasa 2008). To meet this goal, commercial tools such as Ansys-Explicit Dynamics/AUTODYN are used to model the generation of shock and tools such as Statistical Energy Analysis (SEA) and Virtual Mode Synthesis (VMS) are used to analyze the propagated shock.

2 GENERATION OF PYROSHOCK

An explosive bolt or also called pyrotechnic fastener is a fastener that uses pyrotechnic charges which can be initiated remotely. In spacecraft, part of the vehicle must be separated during flight to jettison stages and components that are no longer needed, to uncover equipment, or to deploy payloads. For the final SC/LV separation, clamp band which utilizes one or two explosive bolt is used to break the SC that is bounded together with launch vehicle. These explosive bolts contains two igniters at both ends and with its ignition, high pressure is built inside which creates failure at the notch provided at the bolt. Among the several kinds of explosive bolts found in (Bement 1995), pressure type bolt is chosen in this case as it is also detonated by power cartridge ignition which breaks at the weak point by high pressure. Besides high pressure inside the bolt, the explosion also creates high shock wave that is propagated around the bolt. Therefore, these shock wave and high pressure during separation generates high speed impact between the upper and lower rings and thus the shock is produced. So, this kind of shock level is much necessary to predict as they have the potential to create some serious damage in the payload section. The typical shock measurement as given by (Chang 2002) near clamp-band separation is shown in the Fig. 1. The analysis methodology of this bolt using Explicit Dynamics/AUTODYN is discussed next.

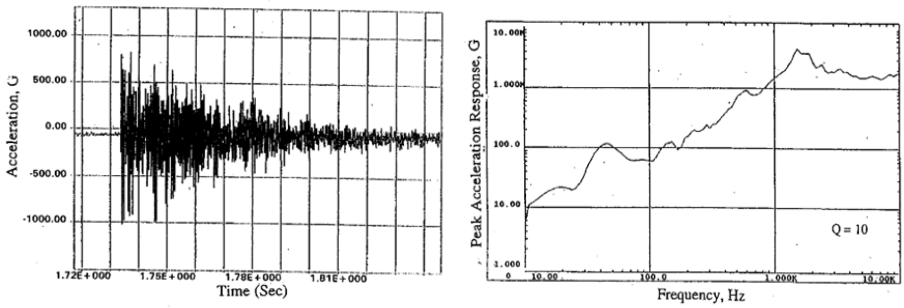

Fig. 1 Typical shock measured near separation plane (Chang 2002)

2.1 Analysis Methodology

Explicit Dynamics module of Ansys is used to model the explosive bolt. The basic Eq. 1 is solved which expresses the conservation of mass, momentum and energy in Lagrange coordinate and with the material model and a set of initial and boundary condition, complete solution of the problem is defined which is acknowledged by (Kim 2011). The explicit dynamics solver uses a central difference time integration scheme and with the computation of forces at the nodes (resulting from internal stress, contact or boundary condition), the nodal acceleration can be derived as Eq. 2. X_i in the equation is the components of nodal accelerations, F_i is the forces acting on the nodes, b_i is the components of body acceleration and m is the mass of the body. With the acceleration determined, the velocities and positions can be obtained by integrating explicitly in time.

$$m\ddot{x} + c\dot{x} + kx = F(\mathrm{t}) \tag{1}$$

$$\ddot{x}_i = \frac{F_i}{m} + b_i \tag{2}$$

As the part of this paper focuses on shock modeling, firstly it is required to perform the 2-D axis-symmetric behavior analysis of an explosive bolt. As such problem definition requires tool that focuses on wave propagation and the interaction with the structure, has explosives material database and coupling between Lagrange and Euler solver is available, explicit dynamics module along with (AUTODYN 2009) is used. This kind of combined program is employed generally for highly nonlinear dynamic problem like blast propagation, ballistic impact etc. as modeling and initial setup is easier in explicit dynamics while expanded/advanced selection of material models and intensive material database of explosives for explosion analysis can be obtained from AUTODYN.

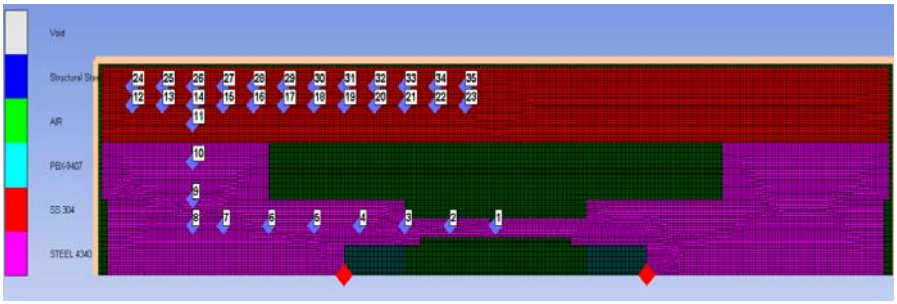

Fig. 2 Pre-analysis AUTODYN model of the bolt

Fig. 2 shows the final pre-analysis model of the bolt along with a part of clamp band. Steel 4340 is used in the bolt part (pink color) as it has an ability to fracture cleanly. The red part is the part of the clamp band and SS304 is used as its material. The two red diamond points are the detonation point while 35 dark blue numbered points are the gauge points which are used to measures the acceleration time history. The cyan colored parts beside two red diamond points are the explosives which is about 6.43g. Also light yellow colored line shows the border of Euler cell where flow out boundary condition is applied. The table 1 below shows the material models such as equation of state, strength, failure and erosion assigned to several materials.

Table 1 Material modes used in AUTODYN

Steel 4340	SS304	RDX
Equation of State: Shock	Equation of State: Shock	EOS: JWL
Strength: Johnson Cook	Strength: Johnson Cook	
Failure: Plastic Strain	Failure: Plastic Strain	Amount:6.43g
Erosion: Failure	Erosion: Failure	

With the completion of analysis, results like material status, pressure contour and several variables like acceleration time history, plastic strain etc. are obtained. The acceleration time history obtained at these gauge points is further used to generate the shock response spectrum. Shock response spectrum is a useful tool for analyzing damage potential of shock pulse as well as test level specification. It is a calculation function which uses acceleration time history as a base excitation as shown in Fig. 3 to of single degree freedom system each with its own natural frequency. Each damping system is typically assumes 5% damping which is equivalent to Q=10.

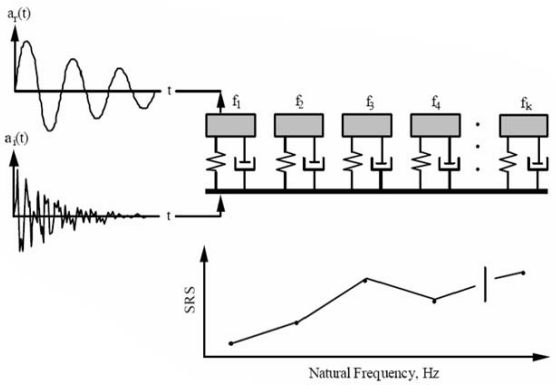

Fig. 3 Shock Response Spectrum based on Acceleration Time History

In the adjoining Fig. 4, the summation of force gives the differential equation of motion as Eq. 3. The relative displacement z= x-y is used to change the expression into Eq. 4. Additional substitution for damping and natural frequency can be made and the Eq. 5 gives the equation of motion for relative response. This equation is solved using convolution integral approach which is then transferred into a series for the case where $\ddot{y}$ is in the form of digitized data. The resulting Eq. 6 is used to calculate SRS in which the required digitized data is provided from the acceleration time history obtained from the gauge point set in the bolt (AUTODYN). The complete derivation can be found in the appendix A of (Irvine 2012).

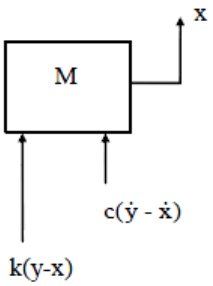

Fig. 4 Free Body Diagram (Irvine 2012)

$$m\ddot{x} + c\dot{x} + kx = c\dot{y} + ky \tag{3}$$

$$m\ddot{z} + c\dot{z} + kx = -m\ddot{y} \tag{4}$$

$$\ddot{z} + 2\xi\omega_n \dot{z} + \omega_n^2 z = -\ddot{y} \tag{5}$$

$$\begin{aligned} \ddot{x}_i &= 2\exp\left[-\xi\omega_n \Delta t\right]\cos\left[\omega_d \Delta t\right]\ddot{x}_{i-1} - \exp\left[-2\xi\omega_n \Delta t\right]\ddot{x}_{i-1} + 2\xi\omega_n \Delta t\ddot{y}_i \\ &+\omega_n \Delta t \exp\left[-\xi\omega_n \Delta t\right]\left\{\left[\frac{\omega_n}{\omega_d}\left(1-2\xi^2\right)\right]\sin\left[\omega_d \Delta t\right] - 2\xi\omega_n \cos\left[\omega_d \Delta t\right]\right\}\ddot{y}_{i-1} \end{aligned} \tag{6}$$

3 PROPAGATION OF PYROSHOCK

Statistical Energy Analysis is a structural acoustic method that arose during 1960 in the aerospace industry to predict the vibrational behavior when designing satellite. The development and use of SEA proved to be good method to predict high frequency loads and the analysis technique has since then been applied, extended and developed for a growing number of applications. Therefore SEA is known to give more accurate predictions with increasing analysis frequency.

In SEA, each system is divided into several physical elements of suitable size. These elements are divided so that the vibro-acoustic characteristics such as damping, excitation and coupling properties are similar. These are termed as subsystem. Once the subsystem is defined, a connection between them is created so that the vibration energy of the system is transferred from directly excited or indirectly excited systems.

$$\begin{bmatrix} P_1 \\ P_2 \\ \vdots \\ P_k \end{bmatrix} = \omega \begin{bmatrix} \left(\eta_1 + \sum_{i=1, i\neq 1}^{k} \eta_{1i}\right) & -\eta_{21} & \cdots & -\eta_{k1} \\ -\eta_{21} & \left(\eta_2 + \sum_{i=1, i\neq 2}^{k} \eta_{1i}\right) & \cdots & -\eta_{k2} \\ \vdots & \vdots & \ddots & \vdots \\ -\eta_{k1} & \cdots & \cdots & \left(\eta_k + \sum_{i=1, i\neq k}^{k} \eta_{ki}\right) \end{bmatrix} \begin{bmatrix} E_1 \\ E_2 \\ \vdots \\ E_k \end{bmatrix} \tag{7}$$

$$\left\{P_{in}\right\} = \omega\left[\eta\right]\left\{E\right\} \tag{8}$$

VMS is currently used in aerospace structure and it is the solution implemented in the PowerSurge program used by AutoSEA shock module for high frequency transient response analysis. It estimates the steady state frequency response magnitude envelope. The source of this frequency response function can result from a steady state SEA solution. The basic idea is that if large number of modes exists at high frequency, the shock can be represented as the peak response from number of local vibration modes with its own natural frequency.

The dynamic behavior of discretized, multi degree of freedom systems subjected to external, time varying point force and moments. The equation of modal analysis can be written as:

$$\left[\tilde{M}\right]\left\{\ddot{\xi}\right\}+\left[\tilde{D}\right]\left\{\dot{\xi}\right\}+\left[\tilde{K}\right]\left\{\xi\right\}=\left[\phi\right]^{T}\left\{F(\mathrm{t})\right\} \tag{9}$$

where

$$\left\{\xi(t)\right\}=\left\{\xi_1(t)\xi_2(t)....\xi_{n_m}(t)\right\}^{T} \tag{10}$$

is the vector of modal displacement response or simply modal vector . M, D and K are the generalized mass, damping and stiffness matrices. If the mode shape vectors $\{\Phi\}_{\mathrm{m}}$ are normalized such that the generalized mass matrix becomes identity matrix, the complex frequency response function (FRF) is calculated as:

$$H_{ij}(i\Omega)=\frac{q_i(i\Omega)}{F_j(i\Omega)}=\sum_{m=1}^{n_m}\frac{\phi_{im}\phi_{ij}}{\left(\omega^2-\Omega^2\right)+2\varsigma_m\omega_m\Omega i} \tag{11}$$

From Eq. 11, the frequency response of any displacement $\mathrm{q_i}$ can be easily determined by adding the contributions for all exciting forces as

$$q_i(i\Omega)=\sum_{j=1}^{n_q}\sum_{m=1}^{n_m}\frac{\phi_{im}\phi_{jm}F_j(i\Omega)}{\left(\omega^2-\Omega^2\right)+2\varsigma_m\omega_m\Omega i} \tag{12}$$

The virtual mode can be roughly defined as the approximations of the actual physical modes and the result of mode synthesis process is a vector containing approximations to the mode shape coefficient products of the ith response and jth force of each virtual mode frequency. Under light damping, all the modes of the system are assumed to be in in-phase, even in a non-resonant condition. Thus, the frequency response magnitude is just a summation of magnitude of each mode response as:

$$\left|H_{ij}(\Omega)\right|=\left|\frac{q_i(i\Omega)}{F_j(i\Omega)}\right|=\sum_{m=1}^{n_m}\frac{\phi_{im}\phi_{jm}}{\sqrt{\left(\omega^2-\Omega^2\right)^2+\left(2\varsigma_m\omega_m\Omega\right)^2}} \tag{13}$$

$$\left|H_{ij}(\Omega)\right|=\left\{\Lambda\right\}^{T}\left\{\Phi\right\}_{ij} \tag{14}$$

Where

$$\left\{\Lambda\right\}=\begin{Bmatrix}\left[\left(\omega_1^2-\Omega^2\right)^2+\left(2\varsigma_1\omega_1\Omega\right)^2\right]^{-\frac{1}{2}}\\ \left[\left(\omega_2^2-\Omega^2\right)^2+\left(2\varsigma_2\omega_2\Omega\right)^2\right]^{-\frac{1}{2}}\\ \vdots\\ \left[\left(\omega_{n_m}^2-\Omega^2\right)^2+\left(2\varsigma_{n_m}\omega_{n_m}\Omega\right)^2\right]^{-\frac{1}{2}}\end{Bmatrix},\ \left\{\Phi\right\}_{ij}=\begin{Bmatrix}\phi_{i1}\phi_{j1}\\ \phi_{i2}\phi_{j2}\\ \vdots\\ \phi_{in_m}\phi_{jn_m}\end{Bmatrix}$$

$$\{\Phi\}_{ij} = \left\{\left[\Lambda\right]^T\right\}^{-1}\left\{\left|H_{ij}(\Omega)\right|\right\} \tag{15}$$

Using Eq. 15, virtual modes $\{\Phi\}_{ij}$ can be calculated using $\left|H_{ij}(\Omega)\right|$ obtained from SEA.

3.1 Shock Propagation Analysis Methodology

In this paper, SEA with shock module is used to construct the model and perform a shock analysis. In a shock module, only one input force can be defined by its time history. Therefore, in the analysis, force tuning work is done until the force time history represents SRS at a given subsystem and the shock is predicted in other subsystems. The methodology from building a model to predicting shock response spectrum is shown in Fig. 5 and the summary of analysis methodology is presented as well.

1) Define System (dividing into different subsystem, defining relationship between them)
2) Evaluate parameters like loss factor, mode count etc.
3) Calculate response (frequency band averaged FRF magnitude)
4) Assume virtual modes in which synthesized FRF approximates the frequency band averaged FRF magnitude.
5) Using synthesized FRF, calculate response in frequency domain.
6) Inverse Fourier transform to get time signal
7) Use the time signal to obtain SRS

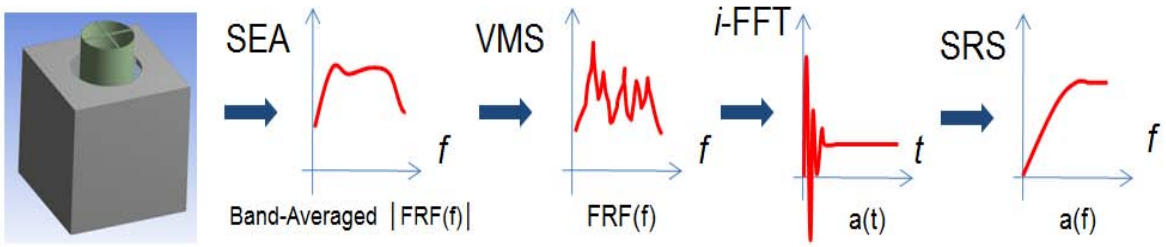

Fig. 5 Steps to analyze the propagated shock

In the present satellite structure as shown in Fig. 14, the shock load as in Fig. 10 is assumed to produce in the lower cylinder where the separation occurs. The simple structure of 24 subsystem is used and the frequency range of interest is chosen as 16~8000 Hz. Since the satellite model is symmetric, the results are computed in one side of a satellite only as shown in Fig. 14. Several assumed loss factors as in Eq. 16~18 are used while defining the system as in (Lee D.O. 2010). As damping loss factor is more significant than the coupling loss factor to obtain better SEA predictions, more concentration is given to properly model the structure with appropriate damping loss factor. VMS is then adopted to predict the satellite's response to the activation of pyrotechnic device which produce high frequency transient load. The half sine force type is used as a shape of the input force. The peak force and the duration of this force are tuned until the predicted shock in the lower cylinder resembles the experimentally

determined SRS. It is seen from the force tuning that the SRS level changes with the change of half sine force magnitude and the shape of the curve with the change in duration of half sine pulse. Also, light damping approximation method is used in which frequency response magnitude becomes the summation of magnitude of each mode response and this calculates the virtual modes. With the calculation of virtual modes, SRS can be generated.

(5% Decreasing Damping)
$$\eta \begin{cases} 0.05 & f \le 500Hz \\ 0.05 * \dfrac{500}{f} & f > 500Hz \end{cases} \quad (16)$$

(1% Decreasing Damping)
$$\eta \begin{cases} 0.01 & f \le 100Hz \\ 0.01 * \dfrac{100}{f} & f > 100Hz \end{cases} \quad (17)$$

(1% Flat Damping)
$$\eta = 0.01 \quad (18)$$

4 RESULTS AND DISCUSSION

This section is focused on presenting results and analyzing them. The first part of this section is dedicated to provide the behavior analysis result of explosive bolt and calculate the shock response spectrum from the acceleration time history which is obtained from AUTODYN. In the second part, the results obtained from SEA used in conjunction with VMS are shown. As mentioned earlier, commercial VA One 2011 with shock module is used to model the satellite and perform shock analysis.

4.1 Behavior Analysis Result of Pyrotechnic Device

The behavior analysis of the explosive bolt is performed with failure model as plastic strain (0.63). Fig. 6 shows the pressure wave propagation and state of bolt at different time. It is observed during the detonation that shock waves of great intensity is produced and as referred by (Luccioni 2003, Luccioni B. 2011), if the explosive is in contact with the solid, it creates intensive pressure wave that can produce the crushing of the material. If it is in contact with the air, a pressure wave is generated that can fracture any masonry and concrete structure. Such effect will produce discontinuities in the material. In order to reduce this type of effects, the erosion model of AUTODYN is used to remove the cells that have reached deformations. When a cell is eliminated, the cell is either be discarded or distributed to the corner nodes of the cell. If its mass is retained, conservation of inertia and spatial continuity of inertia are maintained but the compressive strength and internal energy of the material within the cell are lost. So, like (Luccioni 2011) failure erosion is chosen to show the erosion of the cell after the failure of the element.

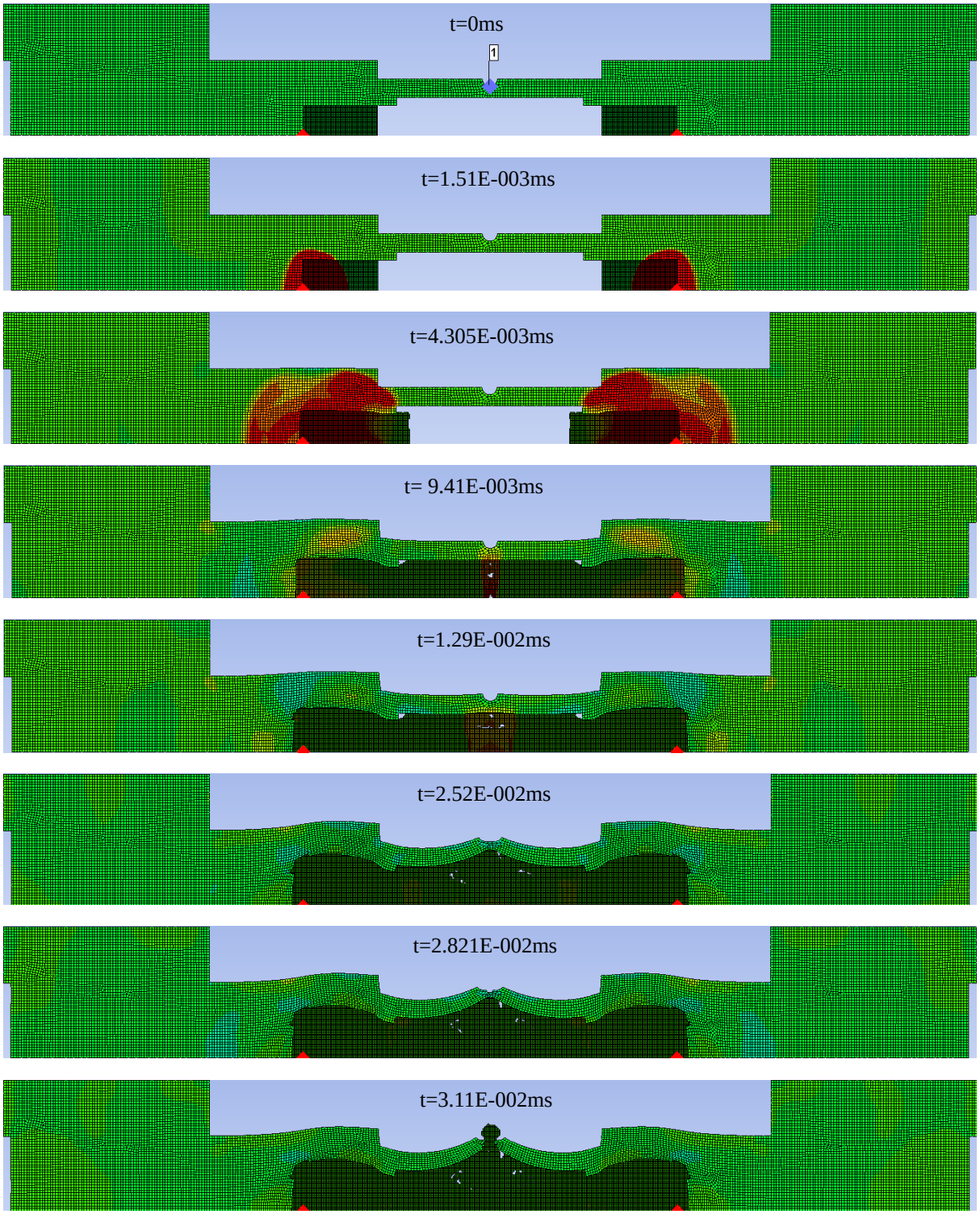

Fig. 6 Separation analysis of pressure bolt used in clamp band system

When the explosion starts at t=0, the shock wave from both end propagates in the bolt while the high pressure builds up at its cavity. At about 0.01ms, high pressure wave starts to build at the mid-section of the bolt where the necking gradually starts and finally fails. The bolt of this kind fails mainly due to the tension failure which is associated to plastic deformation. If the gauge point is set at the separation point as in Fig. 2, the curve of effective plastic strain is obtained which is shown in Fig. 7 (left). From this, it is noticed that the material's ultimate plastic strain (0.63) is reached at about 0.025ms and after that the final separation occurred at 0.032ms due to plastic deformation. The pressure as shown in Fig. 7 (right) displays high pressure created at gauge 3 and 4 and the deformation of the structure there is the result of it. The pressure curve at gauge 1 also shows the bolt failure in 0.032 ms.

As the objective of this section is to estimate the SRS generated during pyrotechnic separation, acceleration time history is obtained from the gauge points set in the structure. As mentioned earlier, a part of the clamp band is also modeled along with the pyrotechnic device so that the acceleration time history can be obtained at that point and SRS can be calculated. So as shown in Fig. 2, from several blue colored gauge points, acceleration data are obtained and SRS's are obtained. The theoretical background on how the SRS is obtained is explained in section 2.5. If the SRS of gauge 3 or 4 is of interest then it is noticed that the shock level at that part is very high and thus SRS will be high. Fig. 1, 8 and 9 shows some of the experimental SRS that are measured at the separation plane. As referred earlier, the SRS magnitude largely depends on the source type and strength, structural type and configuration, and especially the distance from the source to the response point of interest. So, from these figure, the difference in SRS can be noticed although they are all measured at the separation plane. The results in Fig. 8 are measured with three axis accelerometers at 40mm above the clamp band system. Regarding Fig. 1 and 9, it is not mentioned where the SRS is measured. So, the motive at present is to find that gauge point which provides SRS close to these experimental results.

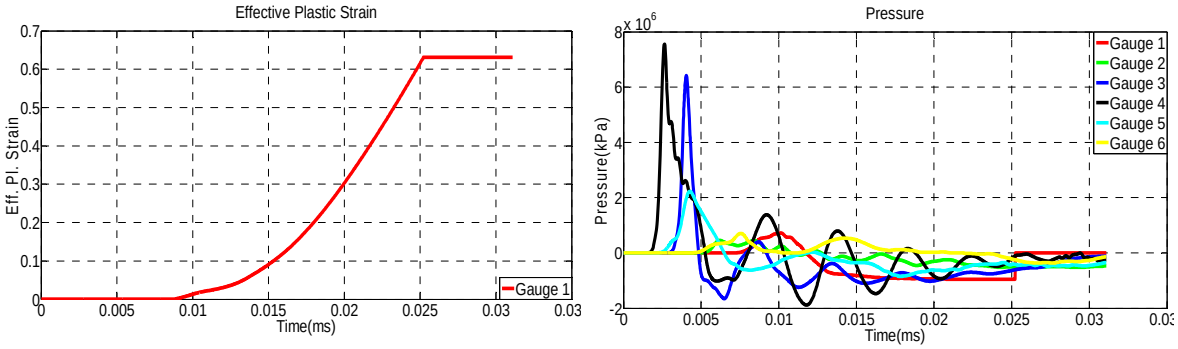

Fig. 7 Effective plastic strain at gauge 1 (left) and pressure curve at gauge 1-6 (right)

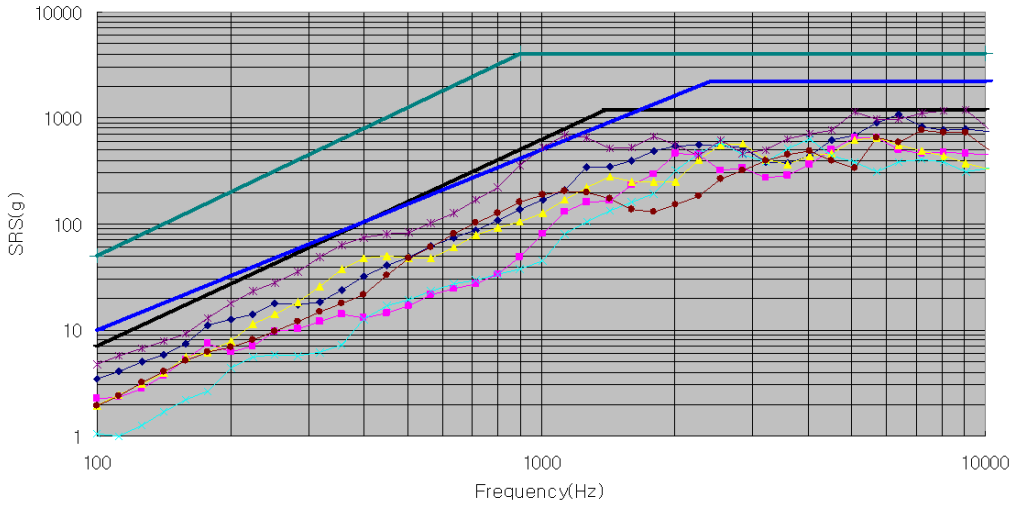

Fig. 8 Experimentally determined SRS (Courtesy of Korea Aerospace Research Institute (KARI))

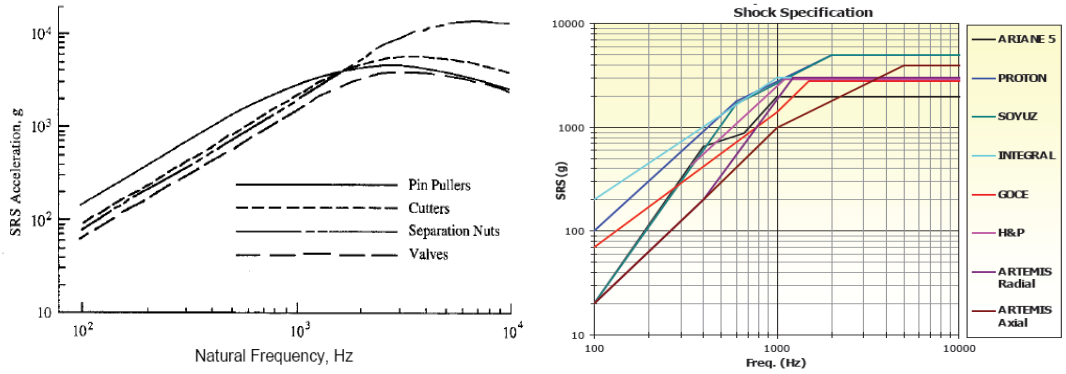

Fig. 9 Near field SRS of different pyrotechnic point source (left - Qinzhong 2004), different satellite (right - Ullio 2006)

The Fig. 10 shows the SRS obtained at different gauge point and if this result is compared with the experimental one in Fig. 8, the curve of gauge 29 and 30 shows close resemblance with the experimentally measured results. At high frequency (>1000Hz), although, the results are in good agreement, there is divergence at mid frequency (<1000Hz). This may be because of the nature of bolt used in this case and other shock characteristics. So, further research is required to evaluate and understand those discrepancies. Next, this result can be used to analyze the shock propagation and so the next section 4.2 is devoted towards it.

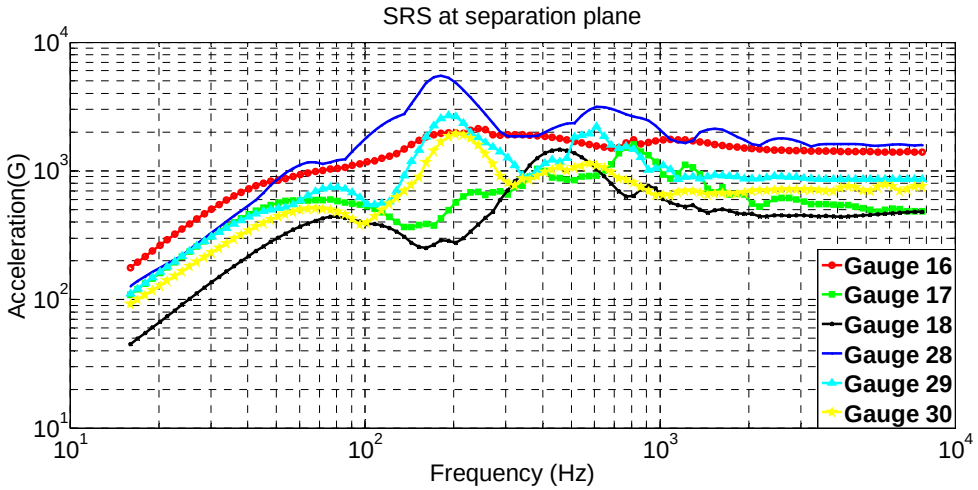

Fig. 10 Numerically obtained SRS at different gauge points

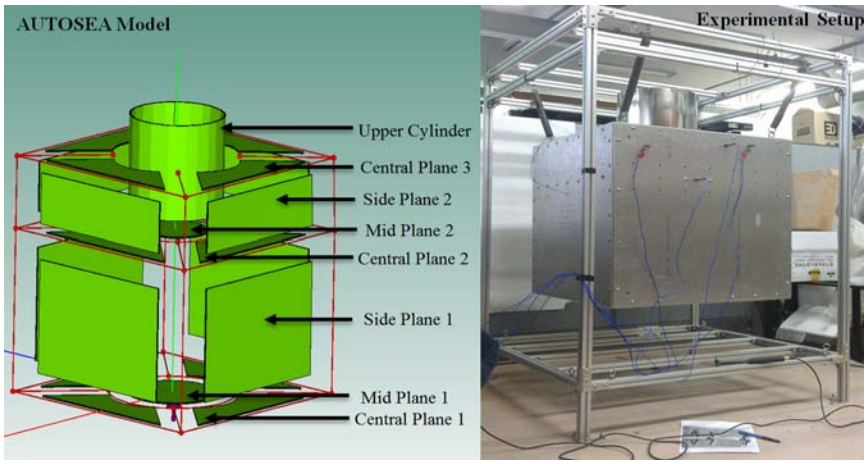

Fig. 11 SEA and experimental satellite model

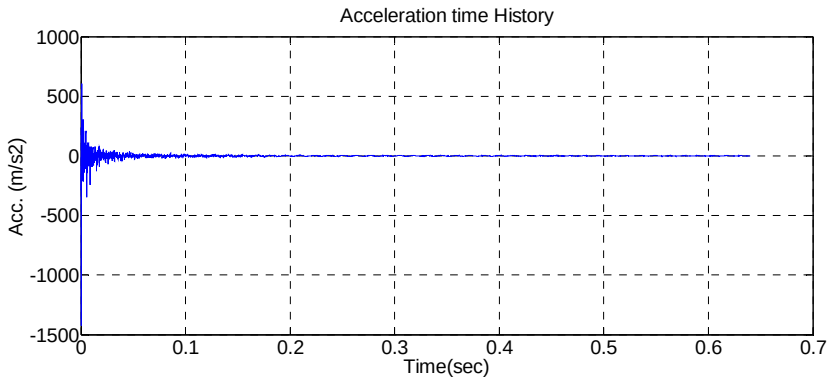

Fig. 12 Impact shock applied at mid plane 1

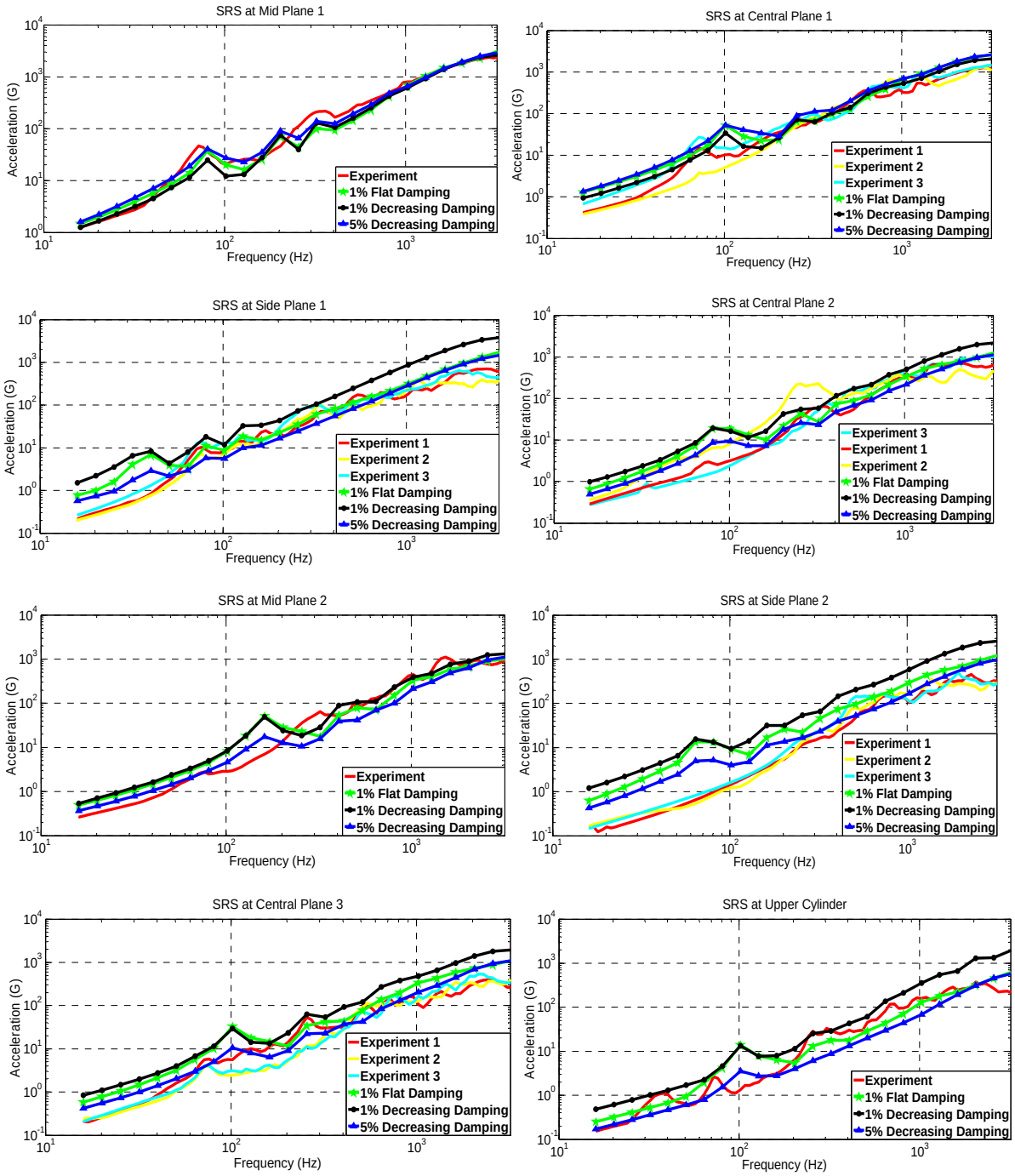

Fig. 13 SRS comparison of experimental and VMS result with various loss factors at different subsystem where shock load is given by impact hammer at mid plane 1

4.2 Shock Propagation Analysis Result

Firstly, for the purpose of partial validation, the experimental shock analysis is performed. As it is difficult and dangerous to provide actual pyroshock load to the satellite model, impact hammer is used instead to excite the structure. Fig. 11 shows

the SEA model with different subsystem and experimental model. The impact shock load as shown in Fig. 12 is given at the mid plane 1 and accelerometers are used at random point of each subsystem to capture the acceleration time signal. From this signal, the SRS are calculated. Also, due to the inability of impact hammer to excite the structure in high frequencies for the determination of loss factors, the experiment is done in the frequency bound of 16~3200Hz with several assumed damping loss factor based on Eq. 16~18. So, in this frequency range, it is observed that the experimental result falls well within the results obtained by using these loss factors. To be more precise, response obtained when using 1% flat damping and 5% decreasing damping are closest to the measured results. All the numerical and experimental results at different subsystem for this frequency bound are shown in Fig. 13. In the case where pyroshock load is given at lower cylinder as shown in Fig. 14, the numerical analysis is performed in the frequency range of 16-8000Hz. Fig. 15 shows the SEA predicted results with assumed loss factors at different subsystem. It is seen from the analysis that SEA/VMS response with 1% flat and 5% decreasing damping are relatively close to each other in almost all the part of the satellite and same is observed with experimental shock analysis results too. So, it may be possible to say that the real response may lie somewhere between the response obtained by these loss factors. The maximum acceleration at lower cylinder is around 1000 G at 3000Hz. With the increase of distance of the receiver end from the source, the decrease of response can be seen. So, at the upper cylinder, the maximum acceleration is 150 G at about 3200Hz. With the increase of damping, huge reduction in magnitude of vibration is noticed and this fact is supported by the difference in response of 1% decreasing and 5% decreasing. Near the shock source, the damping effect is not so significant but the effect is considerable at the upper portion of the satellite.

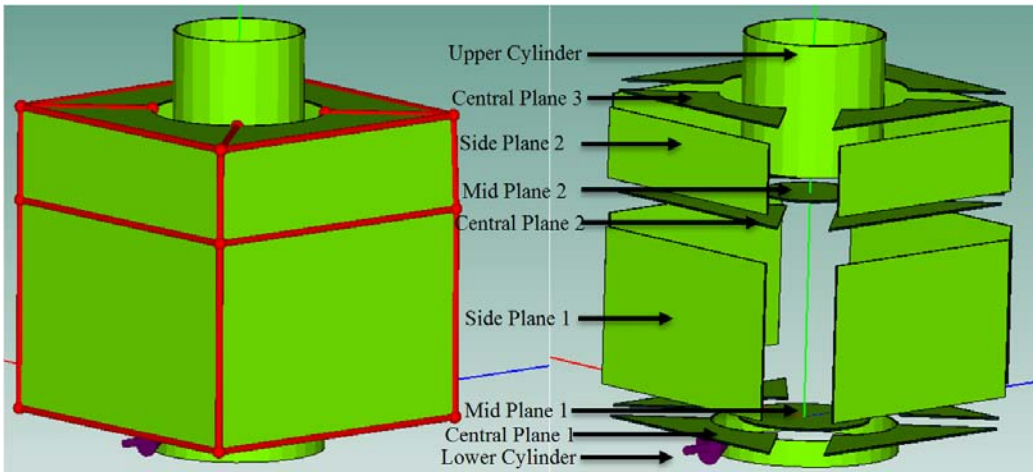

Fig. 14 SEA model with junction (left) and exploded view (right)

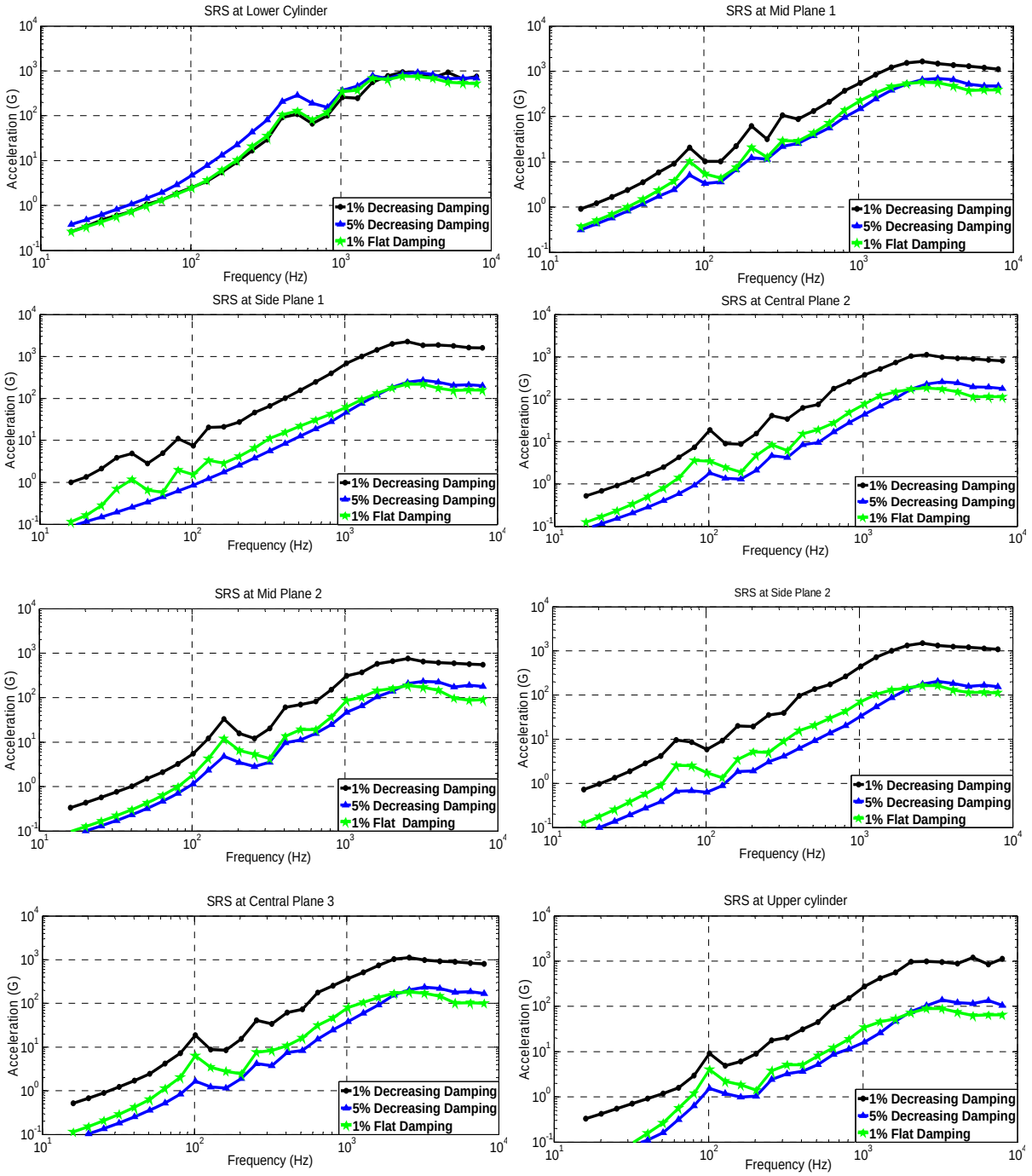

Fig. 15 SRS comparison of predicted result with various loss factors at different subsystem where pyroshock load is given at lower cylinder

5. CONCLUSIONS

Using Ansys-Explicit Dynamics/AUTODYN, the separation phenomena of the pressure type bolt used in clamp band system is studied. Using the gauge points set in different part of the bolt and satellite, acceleration time history is obtained and SRS is predicted at those points. With the change of thickness of the bolt, amount of explosive materials and material properties, shock characteristics is studied and parametric study is performed. Experimentally, it is impossible to measure the near-field SRS. But with the right design of bolt and amount of explosives, it is possible to predict that SRS numerically. Until now, several researchers have provided mid-field SRS and therefore those results are used to validate the numerical result. Though at high frequency, the results are in good agreement, there is some divergence in the results at mid frequency and so further research is required to evaluate that discrepancies.

The shock propagation analysis is performed with SEA/VMS. Several damping loss factor are used and the results are compared. Because of the difficulty in exciting high shock load (same as one produced during actual separation) and high frequency, the experimental analysis is performed in the frequency range of 16~3200 Hz using load given by impact hammer. In this case, it is observed that the results obtained with 1% flat and 5% decreasing damping are closest to the experimental one. Therefore, in the frequency bound of 16-8000Hz, it may be possible that the real response due to pyroshock load may fall within the results predicted by using these loss factors.

ACKNOWLEDGEMENT

This research was supported by NSL (National Space Lab) program through the National Research Foundation of Korea funded by the Ministry of Education, Science and Technology.

REFERENCES

NASA, Preferred reliability practices (1996), “Pyrotechnic shock testing”, Practice No. PT-TE-1408A, May 1996.

Walter, P.L. (2006), Pyroshock Explained, Technical Note TN-23, PCB Piezotronics, 3425 Walden Avenue, Depew, NY 14043-2495, USA.

Lee, Y. J. (2004), “The Interpretation of Separation Mechanism of Ridge-Cut Pyrotechnic device using Simulation Programs”, *Journal of the Korean Society of Propulsion Engineers*, Vol. 8, No. 2, pp. 102~128.

Chang, K.Y. (2002), “Pyrotechnic Devices, Shock Levels and their Applications”, Jet Propulsion Lab, Pyroshock Seminar, *ICSV9*, July 8-11, 2002.

Iwasa, T. and Shi, Q. (2008), “Simplified Estimating Method for Shock Response Spectrum Envelope of V-Band Clamp Separation Shock”, *Journal of Space Engineering*, Ibaraki, Japan, Vol. 1, No. 1, 2008, pp. 46-57ICSV9, July 8-11, 2002.

Bement, L.J. and Schimmel M.L. (1995), “A manual for pyrotechnical design, development and qualification”, *NASA Technical Memorandum 110172*, NASA, Langley Research Centre, Hampton, Virginia.
Kim, G. (2011), ANSYS Workbench Training Manual, WB Explicit STR
AUTODYN-2D. (2009), Version 12.1, User Manual, SAS IP, Inc.
Irvine, T. (2012), “An Introduction to the Shock Response Spectrum”, Revision S, vibrationdata.com.
Lee, D.O., Jang, H.W., Woo, S.H., Kim, K.W., and Han, J.H. (2010), “Shock Response Prediction of a Low Altitude Earth Observation Satellite During Launch Vehicle Separation”, *Int’l J. of Aeronautical and Space Sciences*, 11 (2), 49-57.
Luccioni, B.M., Ambrosini, R.D. and Dansei, R.F. (2004), “Analysis of Building Collapse under Blast Loads”, ELSEVIER, *Engineering Structures* 26, pp. 63~71.
Luccioni, B. and Araoz, G. (2011), “Erosion Criteria for Frictional Materials under Blast Load”, *Asociacion Argentina de Mecanica Computacional*, Mecanica Computacional Vol XXX, pags. 1809-1831.
Shi, Q., Ando, S., Seko, H., Nagahama, K. and Saegusa, H. (2004), “The summarization of pyro-shock testing data and SRS level prediction technology”, *Proceedings of the 5th International Symposium on Environmental Testing for Space Programmes 2004*, Noordwijk, The Netherlands, pp. 549-554.
ULLIO, R. (2006), “AutoSEA Shock Application on Shock Event Simulation – Study Case and Problematics Encountered”, *Vibro-Acoustics Session*, EuroPAM, Toulouse.